9.5

THE EFFECTS OF SUBGRID MODEL MIXING AND NUMERICAL FILTERING IN SIMULATIONS OF MESOSCALE CONVECTIVE SYSTEMS

Tetsuya Takemi * and Richard Rotunno

National Center for Atmospheric Research † Boulder, CO

1. INTRODUCTION

Mesoscale cloud models employ a turbulence closure model in order to represent subgrid-scale (SGS) mixing processes. The turbulence closure models widely used in cloud models, such as the Klemp-Wilhelmson model (Klemp and Wilhelmson 1978), are either a Smagorinsky-type first-order-closure scheme, or a 1.5-order scheme using a prognostic equation of turbulent kinetic energy (TKE). In addition to the SGS mixing, a small amount of background mixing is often employed in order to suppress small-scale computational noise. A common way to achieve this background mixing is to add an explicit scale-selective spatial filter to the model equations; however, this filter cannot differentiate between the physical modes and computational noise, and damps all small-scale perturbations. In some cases physically meaningful small-scale eddies may be suppressed, which can impact the development of mesoscale cloud systems. From the analysis of supercell thunderstorms simulated by the Klemp-Wilhelmson model, Lilly and Jewett (1990) showed that the numerical filter had much more effect on the simulations than the more physically based mixing provided by SGS closure. Therefore, an assessment of subgrid mixing and numerical filtering is crucial for ensuring that a cloud simulation is successful.

The two turbulence closure models mentioned above are formulated as follows: The Smagorinsky-type scheme (Lilly 1962) defines the eddy viscosity coefficient K_m as:

$$K_m = (C_s \Delta)^2 |S| \sqrt{1 - \frac{Ri}{Pr}}, \qquad (1)$$

where S is a deformation tensor, C_s a constant, Δ a measure of the grid scale, Ri the Richardson number, and Pr the turbulent Prandtl number. In the TKE scheme, the eddy viscosity coefficient is given by:

$$K_m = C_k e^{1/2} l, \qquad (2)$$

where C_k is a constant, e is TKE, and l a length scale. The TKE scheme needs another diagnostic equation for determining the TKE dissipation rate ϵ to close the TKE equation:

$$\epsilon = \frac{C_e e^{3/2}}{l}, \qquad (3)$$

where C_e is a constant. The length scale l in (2) and (3) is defined based on the grid scale. In these SGS models, one must determine the proportionality constants C_s, C_k, and C_e. While the values for these constants were derived from theoretical considerations for inertial-subrange, locally isotropic turbulence (Lilly 1966), and have been widely used for simulations of boundary layer flows (e.g., Deardorff 1980), Mason (1994) demonstrated that the results of boundary-layer turbulence simulations depend strongly on C_s: larger C_s gives flows with smoothed features, while reducing C_s suffer from grid-scale perturbations. The eddy viscosity in the Smagorinsky scheme can be easily derived from the TKE prognostic equation; thus, Mason's (1994) argument would also apply to the eddy-viscosity formulation in the TKE scheme, and so, to cloud simulations.

In this study, we investigate the effects of subgrid model mixing and numerical filtering in mesoscale cloud simulations whose grid sizes are order of 1 km (probably far from the inertial subrange), using a newly developed mesoscale cloud model, the Weather Research and Forecasting (WRF) model. For this purpose, we examine the sensitivities of the simulated cloud systems to the SGS constants C_s, C_k, and C_e as well as filter strength. We also examine the sensitivities to the grid spacing for a selected combination of SGS constants. We will address some problems of employing SGS schemes for cloud models, and suggest possible solutions which do not depend on numerical filters. The simulations are performed on squall lines in an idealized situation, which have been extensively investigated in the literature (e.g., Rotunno et al. 1988, Weisman et al. 1988).

2. EXPERIMENTAL DESIGN

The present study mainly focuses on the squall-line evolution in a no-shear environment, which would result in less organized convective cells near the squall-line cold outflow boundary. The WRF model version 1.1.1 is used. The model is run in a three-dimensional domain of 300 km in the x (cross-line) direction and 80 km in the y (along-line) direction extending from the surface to a height of 18 km. The grid sizes are 1 km and 500 m in the horizontal and vertical directions, respectively. Other horizontal grid spacings of 500 m, 2 km, and 4 km are also examined. Open lateral boundary conditions are specified at the x boundaries, and periodic conditions at the y boundaries. The top boundary is rigid lid, while the bottom boundary is free slip. The Kessler warm-rain scheme is used for microphysics parameterization, and the Coriolis parameter is set to zero. A horizontally uniform thermodynamic environment has been created similarly to Weisman et al. (1988). Two initial wind profiles are used: no-shear, no-flow; and the unidirectional shear of 20 $\mathrm{m\,s^{-1}}$ in the lowest 2.5 km. Squall lines are initiated by a y-oriented line thermal (a 1.5 K-maximum potential temperature excess) of across-line radius of 10 km and vertical radius of 1.5 km, placed at the domain center and at a height of 1.5 km, with small random potential temperature perturbations.

We use the third-order upwind differencing scheme for the vertical advection terms in all the simulations. For the horizontal advection terms, we have conducted simulations using three different numerical treatments: third- and fifth-order upwind, and fourth-order centered schemes; however, here we will show only the results using the fifth-order schemes.

The subgrid models used are the Smagorinsky and TKE schemes. The SGS constants derived theoretically by Lilly (1966) are $C_s = 0.23$, $C_k = 0.12$, and $C_e = 0.68$.

* *Corresponding author address*: Dr. Tetsuya Takemi, Department of Global Architecture, Graduate School of Engineering, Osaka Univ., 2-1 Yamadaoka, Suita, Osaka 565-0871; Email: takemi@ga.eng.osaka-u.ac.jp

† The National Center for Atmospheric Research is sponsored by the National Science Foundation.

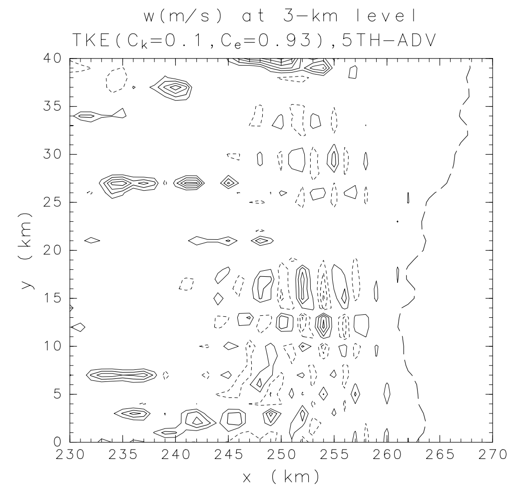

Figure 1: Horizontal cross section of vertical velocity at the 3 km-level, contoured at a 2 $\mathrm{m\,s^{-1}}$ interval at 4 hour. The gust front is also indicated by long-dashed lines. The TKE scheme with $C_k = 0.1$ and $C_e = 0.93$ is used.

Deardorff used $C_s = 0.21$, and most boundary-layer and cloud models employing the TKE scheme use $C_k = 0.1$. Here, we refer to $C_s = 0.2$ and $C_k = 0.1$ as the base SGS constants and examine the influence of varying these constants upon squall-line simulations. In (1) and (2), a length scale must be determined; we define both Δ and l as the geometric-average grid spacing: $(\Delta x \Delta y \Delta z)^{1/3}$, following Klemp and Wilhelmson (1978).

Many cloud models use a fourth-order diffusion (only in the horizontal directions) as a numerical filter. Thus, we also have added a fourth-order diffusion to the WRF model as a numerical filter in order to examine the effects of the filter. According to Klemp and Wilhelmson (1978), we use the non-dimensional filter coefficient $K_4 = 2.4 \times 10^{-3}$ as a weak filter (referred to as FILTER1 here) and, for comparison, $K_4 = 1.2 \times 10^{-2}$ as a strong filter (referred to as FILTER2).

3. SIMULATIONS IN NO SHEAR

3.1 Base SGS constants cases

The simulations with the base SGS constants ($C_s = 0.2$ and $C_k = 0.1$) are considered first to address the issue of using subgrid models without any numerical spatial filters.

Figure 1 shows the horizontal cross section of vertical velocity at the 3-km level and the surface outflow boundary at 4 hours in a 40 km by 40 km area near the right-moving outflow. The subgrid model used here is the TKE schemes ($C_e = 0.93$). The explicit numerical filter is not used in this case. As clearly seen, grid-scale features are widespread behind the gust front, and no well-resolved cells are found. Similar grid-scale noise was seen in the cases using other subgrid models.

In order to examine the cause of the grid-scale features seen in Fig. 1, we have performed a simulation employing neither subgrid model nor additional filter with the fifth-order advection scheme. It should be noted that such a simulation can be conducted because of the robustness of the WRF model. Grid-scale erroneous features are also seen in this simulation (not shown), and comparing this result with that shown in Fig. 1, the simulated fields look similar to each other; thus, the grid-scale noise seen in Fig. 1 results from the erroneous features simulated with neither physical nor numerical dissipation. It can be said that the fifth-order scheme is useful for making the model computationally stable but the implicit smoothing included in the scheme is not enough to resolve sufficiently the convective cells. Thus, the mixing by subgrid models needs to work appropriately in order to represent such cells; however, the simulations suggest that the subgrid mixing is not large enough to smooth the grid-scale noise.

One way to avoid the noisy solution is to add a fourth-order filter and is commonly used in many cloud models that employ leapfrog-time and centered-spatial differencing schemes. However, we seek to find another way to avoid the grid-scale noise by examining the effects of subgrid model mixing and numerical filtering in squall-line simulations.

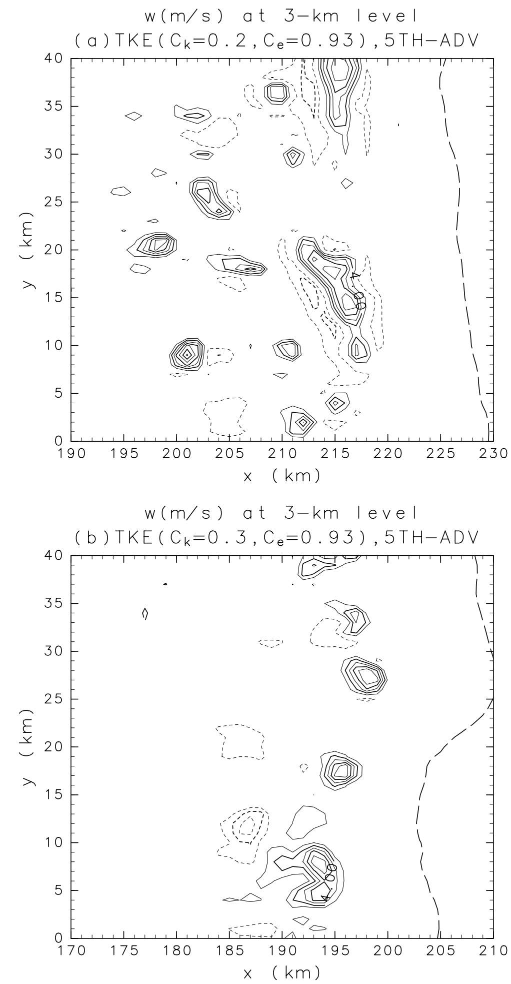

Figure 2: Same as Fig. 1 with (a) $C_k = 0.2$ and (b) $C_k = 0.3$.

3.2 Sensitivities to SGS constants

At first, the effects of varying C_s and C_k are examined. Figure 2 show the horizontal cross section of vertical velocity at the 3-km level around the right-moving cold surface outflow at 4 hours. Increasing the constant C_k beyond the base value, the cells become smoother and well-represented. When the con-

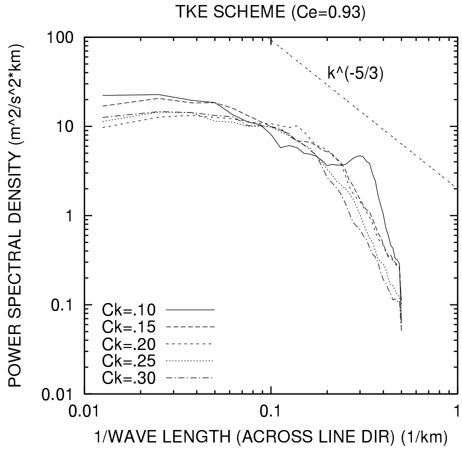

Figure 3: Power spectral density of vertical velocity at the 3-km level for across-line (x) direction obtained using the TKE scheme $(C_e = 0.93)$ with various C_k values. A $k^{-5/3}$ line is also plotted for reference.

stant is further increased to $C_k = 0.3$, the cells look even smoother. These features were also found in the Smagorinsky scheme and the TKE schemes using other C_e values.

To compare more systematically the gross features of the simulations, the power spectral densities in the across-line (x) and along-line (y) directions were computed for the vertical velocity at the 3-km level in a 80 km by 80 km area around the rightward-moving surface outflow. The spectra in each direction were calculated in this domain at each model output time, and averaged over the domain; then the domain-averaged one-dimensional spectra were temporarily averaged during 3-4 hour. Figure 3 shows the power spectral densities in the across-line direction obtained employing the TKE scheme $(C_e = 0.93)$ with C_k varying from 0.1 to 0.3. A spurious buildup of energy is seen in the $C_k = 0.1$ case; however, with $C_k \geq 0.15$ the power in short scales (wavelength less than $10\Delta x$) smoothly decreases with increasing wavenumber. The same behavior of power spectra can be found in other subgrid cases.

To see the difference of the simulated field obtained with the different C_e values, we compared the results using the TKE scheme ($C_k = 0.2$ cases) with $C_e = 0.2$, 0.7, 0.93 (not shown), and found that as C_e decreases the simulated field becomes smoother and small-scale features disappear. However, the effects by changing C_e are not as large as those by changing C_k.

3.3 Sensitivities to numerical filters

To examine the effects of numerical filters, the simulations employing the TKE scheme along with fourth-order filters and, for comparison, employing no subgrid model but only a numerical filter have been performed. The SGS constants are $C_k = 0.1$ and $C_e = 0.93$.

Figure 4 shows the horizontal cross section of vertical velocity at the 3-km level. Adding FILTER1 (Fig. 4a), the noise as seen in Fig. 1 is under control, and the cells appear to be smoothed. Using FILTER2, the simulated cells become further smoothed and most of the small-scale features seen in Fig. 4 disappears (not shown). Comparing the results obtained with and without the TKE scheme (Figs. 4a and b), the structures of the well-resolved cells look similar to each other. This suggests that adding the mixing by the TKE scheme with base

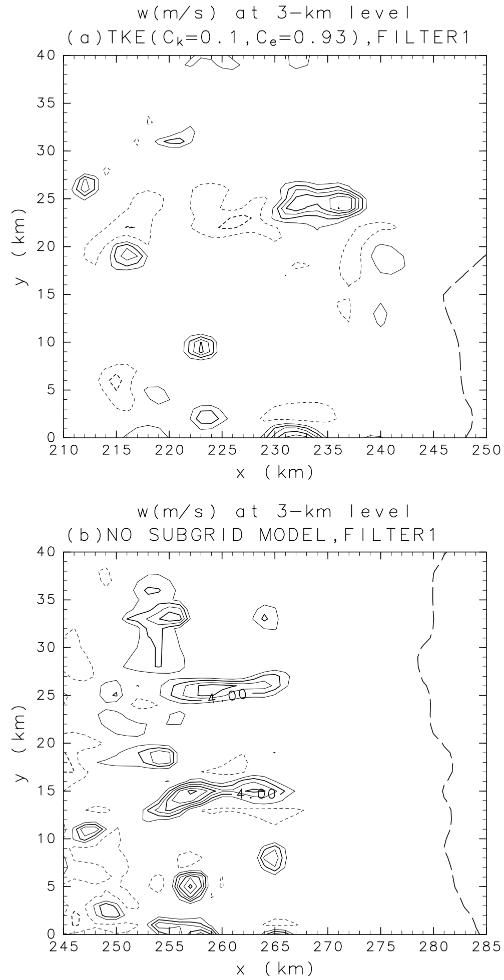

Figure 4: Same as Fig. 1 except for employing (a) the TKE scheme $(C_k = 0.1, C_e = 0.93)$ and weak filter, and (c) no subgrid model with the weak filter.

C_k has a smaller impact on the simulated field than the mixing by the numerical filter.

Since adding the filters resulted in smoother cells, the simulations with the filter may appear to be satisfactory. However, examining the power spectra reveals the difference between the results with and without the filter. Figure 5 shows the power spectral densities of vertical velocity at the 3-km level in the across-line direction for various combination of the TKE scheme and numerical filters. Short wavelengths less than 10 Δx are more rapidly damped with than without the filter. Even though in the no-filter case the eddy viscosity coefficient is increased by a factor of two from the base value, the power at these wavelengths is well-retained. This suggests that numerical filters damp some physically based small-scale eddies.

3.4 Sensitivities to horizontal grid spacing

Here we examine the sensitivities of simulations to horizontal grid spacing, employing the TKE scheme with one set of the optimum SGS constants, i.e. $(C_k, C_e) = (0.2, 0.93)$. As mentioned earlier, we examine a horizontal grid spacing of 500 m, 2 km, and 4 km.

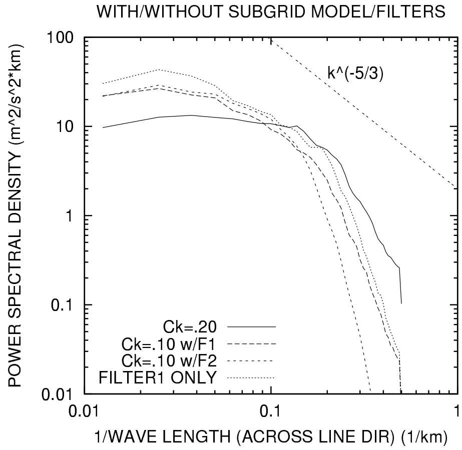

Figure 5: Same as Fig. 3, except the cases employing the TKE scheme ($(C_k, C_e) = (0.2, 0.93)$), the TKE scheme ($(C_k, C_e) = (0.1, 0.93)$) with FILTER1, the TKE scheme ($(C_k, C_e) = (0.1, 0.93)$) with FILTER2, and only FILTER1 without subgrid model.

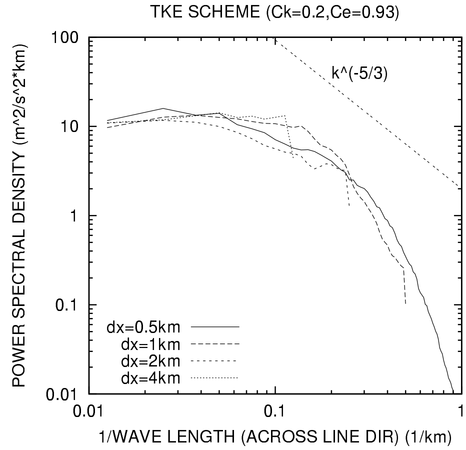

Figure 6: Same as Fig. 3, except the cases with the TKE scheme ($(C_k, C_e) = (0.2, 0.93)$) for different horizontal grid spacings: 500 m, 1 km, 2 km, and 4 km.

The vertical grid spacing is the same as in the above simulations. No fourth-order numerical filter is added.

Comparing the power spectra for the cases with different grid spacing (Fig. 6), all the cases show no spurious buildup of energy at shortest resolved scales, and the power for long scales (more than 10-km wavelength) shows no significant difference with each other.

From these simulations, we can conclude that the optimum SGS constants derived from the 1-km resolution simulations are still valid for the grid spacing ranging from 500 m to 4 km.

4. DISCUSSION AND CONCLUSIONS

From a series of simulations, we have demonstrated the sensitivities of the simulated squall lines to the SGS constants C_s, C_k, and C_e as well as numerical filters. The results have shown that there is an optimum value for C_s and C_k at which the simulated cells are well-resolved. Only the no-shear cases have been shown here, but the simulations in the strong low-level shear environment also showed similar results. We believe that by examining the effects of subgrid mixing and numerical filters the same reasoning as Mason's (1994) can be applied to the present results. The SGS constants should be determined in order to obtain a satisfactory solution for each simulation. It is noted that the present cloud simulations have used a relatively large grid spacing, probably well beyond the inertial subrange, as compared with grid spacings of large-eddy simulations. However, for lack of a better alternative these turbulence-closure schemes will continue to be used; the present study explores some of the consequences of using these schemes with commonly used parameter settings.

The previous studies using cloud models have not noticed the sensitivity to the SGS constants, because most cloud models had to use an artificial numerical filter to smooth out small-scale perturbations. However, as we have shown here, the mixing by numerical filters has a significant influence on the simulated fields. This sensitivity was noticed in previous studies (e.g., Lilly and Jewett 1990), but not investigated systematically. Using the TKE scheme with the widely used $C_k = 0.1$, the subgrid model mixing has an effect much smaller than that of the numerical filter with standard values for the filter coefficient. In order for subgrid model mixing to have an effect and in order not to use numerical filters, the constants C_s and C_k should be increased from the commonly used values.

While we cannot know the best choice of the SGS constants for cloud simulations, we have been able to exclude the obviously bad choices. The present work shows that these choices, along with robust numerics, allow simulations of cloud systems without explicit numerical filters.

ACKNOWLEDGMENT

We would like to thank Joe Klemp, Morris Weisman, and Bill Skamarock for many helpful suggestions and discussions. This work has been done during the first author's visit to NCAR, which was supported by the Ministry of Education of Japan and NCAR.

REFERENCES

Deardorff, J. W., 1980: Stratocumulus-capped mixed layers derived from a three-dimensional model. *Bound.-Layer Meteor.*, **18**, 495-527.

Klemp, J. B., and R. B. Wilhelmson, 1978: The simulation of three-dimensional convective storm dynamics. *J. Atmos. Sci.*, **35**, 1070-1096.

Lilly, D. K., 1962: On the numerical simulation of buoyant convection. *Tellus*, **14**, 148-172.

Lilly, D. K., 1966: On the application of the eddy viscosity concept in the inertial sub-range of turbulence. Manuscript No.123, National Center for Atmospheric Research, Boulder, CO, 19 pp.

Lilly, D. K., and B. F. Jewett, 1990: Momentum and kinetic energy budgets of simulated supercell thunderstorms. *J. Atoms. Sci.*, **47**, 707-726.

Mason, P. J., 1994: Large-eddy simulation: A critical review of the technique. *Quart. J. Roy. Meteor. Soc.*, **120**, 1-26.

Rotunno, R., J. B. Klemp, and M. L. Weisman, 1988: A theory for strong, long-lived squall lines. *J. Atmos. Sci.*, **45**, 463-485.

Weisman, M. L., J. B. Klemp, and R. Rotunno, 1988: Structure and evolution of numerically simulated squall lines. *J. Atmos. Sci.*, **45**, 1990-2013.